Nonlinear Tactile Estimation Model based on Perceptibility of Mechanoreceptors improves Quantitative Tactile Sensing

Momoko Sagara (sagarapeach@keio.jp)
Keio University: Keio Gijuku Daigaku https://orcid.org/0000-0002-6425-4988
Lisako Nobuyama
Keio University - Yagami Campus: Keio Gijuku Daigaku - Yagami Campus
Kenjiro Takemura
Keio University: Keio Gijuku Daigaku

Research Article

Keywords: Tactile estimation, nonlinear regression, sensory evaluation, mechanoreceptors, tactile sensor

Posted Date: January 10th, 2022

DOI: https://doi.org/10.21203/rs.3.rs-1213598/v1

Abstract

Tactile sensing has attracted significant attention as a tactile quantitative evaluation method because the tactile sensation is an important factor while evaluating consumer products. While the human tactile perception mechanism has nonlinearity, previous studies have often developed linear regression models. In contrast, this study proposes a nonlinear tactile estimation model that can estimate sensory evaluation scores from physical measurements. We extracted features from the vibration data obtained by a tactile sensor based on the perceptibility of mechanoreceptors. In parallel, a sensory evaluation test was conducted using 10 evaluation words. Then, the relationship between the extracted features and the tactile evaluation results was modeled using linear/nonlinear regressions. The best model was concluded by comparing the mean squared error between the model predictions and the actual values. The result implies that there are multiple evaluation words suitable for adopting nonlinear regression models, and the average error was 43.8% smaller than that of building only linear regression models.

Introduction

Since tactile sensation is one of the most important factors when evaluating a consumer product [1-4], quantitative evaluation methods for tactile sensation are in high demand in product development. In general, a sensory evaluation test is employed to quantify tactile sensations; however, it requires many subjects to participate in a survey, which is costly and time-consuming. As an alternative to sensory evaluation tests, tactile estimation using physically acquired quantitative data, or *tactile sensing*, has attracted significant attention.

Some previous studies have focused on developing tactile sensors [5-15]. Fishel et al. [5] developed a tactile sensing finger, *BioTac*, which can detect force, vibration, and heat transfer. Lin et al. [6] developed a human skin-inspired piezoelectric flexible multifunctional tactile sensor that can detect and distinguish the magnitudes, positions, and modes of diverse external stimuli, including slipping, touching, and bending the tactile sensor. Zheng et al. [7] developed a magnetostrictive tactile sensor based on a Galfenol cantilever. The surface properties, including roughness and slipperiness of an object, can be obtained when the sensor slides on an object's surface. Most tactile sensor development approaches are based on a robotic strategy, which pays little attention to human perceptibility.

Another approach is to extract meaningful information from vibration data obtained by tracing a simple vibration sensor on an object [16-22]. Because the four types of mechanoreceptors in our body have different frequency characteristics [23-25], they work as filters for vibration stimulations on the skin. This means that the meaningful information for humans is not the entire vibration data but is hidden in the vibration data. Previous research [16-19] focused on extracting meaningful information; we believe that it is quite promising because the information or feature quantities are often extracted based on the characteristics of human mechanoreceptors. By doing so, it becomes possible to interpret tactile sensation based on human perceptive characteristics. These extracted features provide helpful information for engineers in designing a product. Contrastingly, to push this approach forward from mere

basic knowledge to extract feature quantities to a practical level, it is essential to show how to take full advantage of extracted features in the tactile estimation process in which the nonlinearity of human perceptive nature [26-27] is taken into account. This study aims to demonstrate how nonlinear modeling contributes to the tactile estimation process, together with the further expansion of the feature extraction procedure.

Methods

Strategy of tactile estimation modeling

The structure of this study is shown in Figure 1 to demonstrate the effectiveness of the nonlinear modeling of tactile estimation. First, we conducted a sensory evaluation test. In parallel, a tactile sensing system is developed, including a newly designed tactile sensor. The vibration data while the sensor traces on a sample are acquired, followed by feature extraction based on the perceptibility of mechanoreceptors. Then, we develop several model candidates with or without nonlinearities, whose inputs and outputs are the extracted features and sensory evaluation scores, respectively. The mean squared error between the model predictions and the actual values is compared to determine the most effective model.

Target samples

As shown in Figure 2 (a), eight plastic plates were used in this study as target samples. The plates had different surface patterns. The differences are shown in Table S1 as the arithmetic average roughness of the samples, R_a, and the arithmetic average swell, W_a, measured using DektakXT (Bruker Corporation, Billerica, MA, USA). The dynamic friction coefficient, μ', was measured using KES-SE with a 10 mm^2 piano-wire sensor (Kato Tech Co. Ltd., Kyoto, Japan), as shown in Figure 2 (b).

Sensory evaluation test

To quantify the tactile sensations, a sensory evaluation test was conducted with human subjects, performed under 24.6 ± 1.0 ℃ and 41.3 ± 4.5% relative humidity with the participation of 35 healthy adults (21 males and 14 females) aged 22.2 ± 1.1 (between 21 and 25) years old. We employed a semantic differential method with a seven-step unipolar scale for the Japanese adjectives listed in Table S2. Before the evaluation, the subjects were free to touch all the samples to understand the variety of the samples. During the test, each sample was placed in a box to exclude visual information. The subjects were allowed to evaluate the samples in random order. In addition, the evaluation words were given to each participant in random order to prevent a possible order effect from occurring. The test protocol was approved by the Bioethics Board of the Faculty of Science and Technology, Keio University. The subjects received a thorough explanation of the test methods in advance and then signed an informed consent form before participating in the study.

To identify trends in the subjects' responses, the subjects were classified using cluster analysis using the Python library, Scipy. The scores for all evaluated words were considered in the cluster analysis. The

Euclidean distance was used as the distance function, and the Ward method was employed.

For the analysis of tactile sensation, the evaluation words were analyzed by principal component analysis (PCA) for each cluster of subjects based on the evaluation scores using SPSS (Version 22, International Business Machines Corp., Armonk, NY, USA). The conditions for extracting the principal components (PCs) include the criteria that the eigenvalue of each PC should be greater than unity.

Vibration measurement system and procedure

We developed a tactile sensing system capable of detecting vibrations while a tactile sensor runs over a sample. Figure 3 shows the images of the tactile sensor and an overview of the tactile sensing system. A cylindrical shaft converts vertical displacement into the strain of a leaf spring with two strain gauges (KFGS-03-120-C1-23-N30C2, Kyowa Electronic Instruments Co. Ltd., Tokyo, Japan) glued on both sides to detect vibrations when a silicone rubber pad traces a sample surface. The hardness of the silicone rubber pad was designed to be equivalent to that of a human finger. Figure S1 shows a comparison of hardness between the forefinger pad and the developed sensor measured using a durometer TYPE OO (GS-754G, Teclock Co. Ltd., Nagano, Japan). The results of the Student t-test showed no significant differences between the two.

A coating material (X-93-1755-1, Shin-Etsu Chemical Co. Ltd., Tokyo, Japan) was adhered to the surface of the silicone rubber pad. The outputs from the strain gauges were acquired using a dynamic strain amplifier (DPM-913B, Kyowa Electronic Instruments Co. Ltd., Tokyo, Japan). The relationship between the output of the strain gauge (V) and the vertical deformation of the tactile sensor (d) is shown in Figure S2. From the figure, we can obtain the transformation equation with linear regression as

$$d = -1409.4V + 710.35 \#(1)$$

As shown in Figure 3 (c), the tactile sensor was fixed to a traction arm of the static and dynamic friction measuring instruments (TL201Ts, Trinity-Lab. Inc., Tokyo, Japan). Upon testing, the normal force N between the tactile sensor and the sample can be adjusted by placing weights on the traction arm. As the sample table of the TL201Ts moves horizontally, the tactile sensor runs over a sample. In addition, a force sensor connected to the traction arm detects the tangential force F.

The vibration information measurement conditions were as follows: the tracing speed and distance of the tactile sensor were 10 mm/s and 30 mm, respectively. The normal force, N, applied between the tactile sensor and sample was 0.49 N. Measurements were repeated 11 times per sample.

Data processing methods

There are four mechanoreceptors in the glabrous skin, as shown in Figure S3: Meissner corpuscles (FA I), Pacinian corpuscles (FA II), Merkel disks (SA I), and Ruffini endings (SA II) [22-24]. They respond to mechanical stimuli applied to the skin and then fire nerve impulses to the neuron. The physiological threshold of the amplitude of stimulation for firing against the frequency has been reported for each

receptor, as summarized in Figure S4. Based on this, we can approximate the threshold line, *L*, on the logarithmic chart for each mechanoreceptor as

$$L_{FAI} = \begin{cases} -17.22\log f + 53.91, & \text{if } 0.5 \le f \le 10.13 \\ -12.12\log f + 48.78, & \text{if } 10.13 < f \le 14.73 \\ 0.2373\log f + 34.34, & \text{if } 14.73 < f \le 67 \end{cases} \quad (2)$$

$$L_{FAII} = \begin{cases} -38.64\log f + 64.57, & \text{if } 20 < f \le 237.64 \\ 24.93\log f - 86.48, & \text{if } 237.64 < f \le 800 \end{cases} \quad (3)$$

$$L_{SAI} = \begin{cases} -10.90\log f + 32.77, & \text{if } 0.5 \le f \le 20.55 \\ 9.195\log f + 6.390, & \text{if } 20.55 < f \le 120 \end{cases} \quad (4)$$

$$L_{SAII} = \begin{cases} -17.22\log f + 53.90, & \text{if } 0.5 \le f \le 10.13 \\ -12.12\log f + 48.78, & \text{if } 10.13 < f \le 128.51 \\ -0.6747\log f + 24.64, & \text{if } 128.51 < f \le 400 \end{cases} \quad (5)$$

where L_{FAI}, L_{FAII}, L_{SAI}, and L_{SAII} are the thresholds for FA I, FA II, SA I, and SAII, respectively, and *f* is the frequency of the vibration stimulus. Each mechanoreceptor fires when the intensity of the mechanical stimulus surpasses the corresponding threshold line.

The vibration data acquired by the vibration measurement system (Figure 3) were compared with the above-mentioned threshold lines in the frequency domain to extract meaningful information for tactile estimation as follows: First, the acquired output from the strain gauges was converted to vertical displacement using Equation (1), resulting in the vibration data in the time domain. Then, we transformed the vibration data from the time domain to an amplitude spectrum in the frequency domain using fast Fourier transformation (FFT), implemented in MATLAB (MATLAB 2020a, Math Works Inc., Natick, MA, USA) at a sampling frequency of 10 kHz mediated with a Hamming window, to obtain the vibration data in the frequency domain. Figure 4 shows a conceptual diagram of the extraction of feature values. The colored area between the lowest threshold and the measured vibration data corresponds to the firing status of the mechanoreceptors. This study considers the combination of firing receptors and divides the entire area into eight sub-areas, D_i, as shown in Figure 4. The subscript *i* represents the mechanoreceptors that are supposed to fire in the corresponding frequency range. Note that D_i could be zero when the vibration data are always lower than the thresholds. Detailed formulas for calculating each feature are provided in the Supplementary Material.

Tactile estimation models

We performed a regression analysis to predict the principal component scores for each cluster using the features extracted from the vibration data, D_i, and the dynamic friction coefficient, μ', using the Python

library and state models. Considering that the human tactile perception nature has nonlinearity [25], we developed four types of linear/nonlinear regression models:

$$Linear: y = \beta_0 + \sum_{i=1}^{p} \beta_i x_i \quad (6)$$

$$Logarithmic: y = \beta_0 + \sum_{i=1}^{p} \beta_i \log\left(x_i\right) \quad (7)$$

$$Interaction: y = \beta_0 + \beta_1 x_i + \beta_2 x_j + \beta_3 x_i x_j \quad (8)$$

$$Polynomial: y = \beta_0 + \sum_{i=1}^{a} \beta_1 x_1^i \quad (9)$$

where x_i and x_j are the explanatory variables, that is, D_i and μ'. y is the objective variable, that is, the PC score. β_i represents the coefficients to be determined. In the interaction model, any two explanatory variables were chosen to build the model, that is, ${}_6C_2$ = 15 types of models were built for one objective variable.

The explanatory variables were introduced using the brute-force method. A regression model was constructed using data obtained from seven out of eight samples. The data for the remaining samples were used to validate the developed regression model. This process was repeated eight times, that is, all samples were used for validation. The model with the lowest error was selected as the best model for each PC in each cluster.

For comparison, we also conducted regression analyses using the feature extraction methods reported in a previous study [17]. In other words, a total of eight regression equations were constructed for one objective value by combining two types of feature extraction methods and four types of models, and the name of each regression model was defined, as shown in Table 1. Previous research [17] only considered three features extracted from the vibration data and used linear regression analysis. Thus, A-1 is the method reported in a previous study [17], and the other models were newly constructed in this study.

Table 1
Classification of the regression models based upon the feature extraction method and model type

		Feature extraction method	
		Previously reported method [17]	Proposed method
Model type	Linear	A-1	B-1
	Logarithmic	A-2	B-2
	Interaction	A-3	B-3
	Polynomial	A-4	B-4

Results And Discussion

Sensory evaluation results

As a result of cluster analysis, the subjects were mainly classified into Cluster 1 (10 subjects) and Cluster 2 (25 subjects), as shown in Figure 5. PCAs were performed on the clusters. The results show two PCs extracted for Cluster 1 and three for Cluster 2, as shown in Table 2. The cumulative contribution rates of the PCA results for Clusters 1 and 2 were 73.2% and 59.7%, respectively. The average PC scores for each sample were considered as objective variables in the following regression analysis.

Table 2
The result of principal component analysis

Evaluation word	Principal component load				
	Cluster 1		Cluster 2		
	PC 1	PC 2	PC 1	PC 2	PC 3
Smooth	**-0.933**	-0.055	**-0.646**	0.186	**-0.517**
Sticky	**0.913**	0.136	**0.695**	0.300	-0.257
Pasty	**0.872**	0.120	**0.724**	0.385	0.088
Feel friction-drag	**0.877**	0.000	**0.741**	0.220	0.099
Moisten	**0.840**	0.236	0.466	0.371	0.276
Sleek	**-0.845**	0.196	**-0.617**	0.356	-0.033
Slippery	**-0.561**	0.427	-0.200	**0.725**	0.075
Velvety	-0.215	**0.836**	**-0.603**	0.319	0.318
Fine	-0.048	**0.810**	-0.452	0.356	**0.507**
Rough	-0.188	**-0.772**	-0.011	**-0.673**	0.461
Eigen value	5.50	2.26	3.18	1.79	1.00
Contribution rates (%)	50.4	22.8	26.3	18.8	14.6
Cumulative contribution rates (%)	50.4	73.2	26.3	45.1	59.7

Bold letters indicate evaluation words with an absolute value of PC loadings of 0.5 or higher.

Feature values extracted from vibration

The features corresponding to the eight sub-areas in Figure 4 were calculated, as shown in Figure 6. As indicated, all the features have different trends among the samples, suggesting that these features

extracted from vibration data could possibly explain the differences in the samples. A one-way analysis of variance showed that there were significant differences ($p < 0.05$) between samples for $D_{SAISAIIFAI}$, D_{ALL}, $D_{SAISAIIFAII}$, D_{FAII}, and $D_{SAIIFAII}$. Therefore, these five features for each sample were considered as index variables in the following regression analysis.

In addition, the three types of features calculated based on the feature calculation method of a previous study [17] are shown in Figure S5.

Regression analysis

Using the features and the dynamic friction coefficient μ' as index variables, we performed regression analysis to estimate the results of the sensory evaluation. The type of model that showed the lowest error for each principal component and its values are shown in Table 3, with the smallest error among all models for each PC shown in bold. The relationship between the values predicted by the model with the smallest error and the measured values is shown in Figure 7.

Table 3
The average error of each regression models

Cluster	Principal component	Model							
		A-1	A-2	A-3	A-4	B-1	B-2	B-3	B-4
Cluster 1	PC1	0.134	0.115	0.876	0.138	0.052	**0.018**	0.876	0.061
	PC2	0.539	0.506	1.133	0.795	0.545	0.535	**0.338**	0.451
Cluster 2	PC1	0.328	0.231	0.211	0.426	0.227	**0.209**	0.542	0.307
	PC2	0.268	0.325	0.303	0.733	**0.046**	0.048	0.321	0.138
	PC3	0.418	0.416	0.688	0.360	0.386	0.385	0.441	**0.337**
Bold letters indicate the model with the lowest error for each PC.									

As shown in Table 3, the B-*n* models, in which the features were extracted by the proposed method, had the lowest error among all PCs. This implies that considering the combination of firing receptors would improve the accuracy of tactile estimation. As can be seen, the linear regression model (B-1) is effective only for PC 2 in Cluster 2, whereas the nonlinear models (B-2, B-3, B-4) are effective for the other PCs. In other words, these results suggest the effectiveness of considering nonlinear models. When the tactile sensation was estimated by the method of a previous study [17], that is, when only the A-1 models were constructed, the mean error of all five PCs was 0.337. In contrast, when both linear and nonlinear models are considered using the features proposed in this study, the average error (for the models shown in bold in Table 3) is 0.190. This is a 43.8% smaller error than that using the A-1 models.

PC2 in Cluster 2, where the linear model was effective, had evaluation words with high principal component loadings such as “Slippery” and “Rough”, as shown in Table 2. This implies that the roughness represented by PC2 in Cluster 2 was perceived. Furthermore, we found that the logarithmic model was effective for PC1 in both Cluster 1 and Cluster 2. Both principal components have “Smooth,” “Sticky,” “Pasty,” “Feel friction-drag,” and “Sleek” as the evaluation words with an absolute value of principal component loadings of 0.5 or higher. They are thought to represent similar tactile sensations, such as smoothness. Thus, the results imply that we do not perceive vibration stimuli linearly but logarithmically when perceiving smoothness regardless of the cluster. Contrastingly, PC2 in Cluster 1 and PC3 in Cluster 2, which represent similar tactile sensations, were effectively modeled by different types of models: interaction model and polynomial model, respectively. This difference may be due to the different perceiving nature of each cluster. Therefore, to make the most of the extracted features in tactile estimation, it is necessary to combine different types of models for different PCs or evaluation words.

The regression equations for constructing the model with the smallest error are shown in Eqs. (10) to (14).

$$y_{C1PC1} = -4136 + 5.544\log\left(D_{SAISAIIFAI}\right) - 98.20\log\left(D_{SAIIFAII}\right) + 466.3\log\left(D_{FAII}\right) + 0.9490log(\mu) \quad (10)$$

$$y_{C1PC2} = 1.828D_{SAIIFAII} - 3.5 \times 10^{-4}D_{SAIIFAII}^{2} + 1.69 \times 10^{-8}D_{SAIIFAII}^{3} \quad (11)$$

$$y_{C2PC1} = -16.88 + 2.856\log\left(D_{SAISAIIFAI}\right) + 1.114\log(\mu) \quad (12)$$

$$y_{C2PC2} = -94.98 + 4.824 \times 10^{-3}D_{SAISAIIFAII} - 4.270 \times 10^{-3}D_{ALL} + 8.772 \times 10^{-3}D_{SAIIFAII} \quad (13)$$

$$y_{C2PC3} = 4911 - 2.237D_{SAISAIIFAII} - 0.4723D_{SAIIFAII} + 2.151 \times 10^{-4}D_{SAISAIIFAII}D_{SAIIFAII} \quad (14)$$

Note that y_{CiPCj} is the principal component score of the *jth* PC of Cluster *i*. The coefficient of determination R^2, the adjusted coefficient of determination R'^2, and the p-values of each regression equation are shown in Table 4. This indicates that the regression equations constructed for PC2 in Cluster 1 and PC3 in Cluster 2 were insignificant, with a significance probability of 5%. In conjunction with the results in Table 3, we can see that the errors of the two models are relatively large (more than 0.3), although they are smaller than those of the previously reported models. Measuring any additional physical quantities may improve the estimation of these tactile sensations.

Table 4
Summary of the constructed regression equations

Cluster	Principal Component	Equation	R^2	$R^{\prime 2}$	p
Cluster 1	PC1	(10)	0.995	0.986	0.000854
	PC2	(11)	0.458	0.241	0.217
Cluster 2	PC1	(12)	0.837	0.772	0.0107
	PC2	(13)	0.935	0.887	0.0077
	PC3	(14)	0.308	-0.211	0.651

In the following, we will examine which features effectively explain PC1 in Cluster 1 and PC1/PC2 in Cluster 2, for which statistically significant regression equations were constructed ($p < 0.05$). Table 5 shows the standard regression coefficients, β', and their p-values for each variable. PC1 in Cluster 1 and PC1 in Cluster 2, which represent similar tactile sensations of smoothness, have $\log\left(D_{SAISAIIFAI}\right)$ and $\log(\mu)$ as explanatory variables. From the calculated range of $D_{SAISAIIFAI}$, the vibration between 0.5 Hz to 20 Hz and the dynamic friction coefficient contribute the most to the smoothness. This is evident from the large absolute value of the standard regression coefficient of $\log\left(D_{SAISAIIFAI}\right)$ as shown in Table 5. In addition, PC1 in Cluster 1 included other explanatory variables, $\log\left(D_{SAIIFAII}\right)$ and $\log\left(D_{FAII}\right)$, as well. PC2 in Cluster 2, which represents the roughness, shows that the standard regression coefficients of D_{ALL} and $D_{SAIIFAII}$ are approximately the same. From the range of the feature value calculation, it can be said that vibrations between 20 Hz and 67 Hz are negatively, and vibration between 97.44 Hz and 400 Hz are positively correlated with roughness.

Table 5
Standard regression coefficients for each variable

Objective variable	Explanatory Variable	β'	p
y_{C1PC1}	$\log\left(D_{SAISAIIFAI}\right)$	0.797	0.004
	$\log\left(D_{SAIIFAII}\right)$	-0.426	0.011
	$\log\left(D_{FAII}\right)$	0.469	0.018
	$\log(\mu)$	0.438	0.013
y_{C2PC1}	$\log\left(D_{SAISAIIFAI}\right)$	0.515	0.039
	$\log(\mu)$	0.645	0.018
y_{C2PC2}	$D_{SAISAIIFAII}$	0.357	0.072
	D_{ALL}	-0.787	0.005
	$D_{SAIIFAII}$	0.798	0.005

Conclusions

The estimation of tactile sensation is necessary for the development of products to improve additional values. For this purpose, we developed a tactile sensing system capable of detecting vibrations while a sensor runs over a sample. From the vibration obtained, we proposed methods to estimate the firing values of mechanoreceptors based on the human tactile perception mechanism. Simultaneously, we conducted sensory evaluations to obtain the sample scores for different evaluation words and extracted principal components for the tactile sensation of samples for the cluster divided by response tendency. Then, the relationship between the extracted features and tactile evaluation scores was modeled by linear and nonlinear regressions. The best model was determined by comparing the estimation errors. In conclusion, the results suggest the effectiveness of the feature extraction method proposed in this study and the reduction of error by considering nonlinear models. In addition, the obtained regression equations reveal the physical quantities that contribute to the estimation of smoothness and roughness. In contrast, the probability of some models is not small enough for quantitative tactile estimation. Measuring additional physical quantities may improve the estimation of these tactile sensations.

Abbreviations

PC
Principal component

Declarations

Availability of data and materials

The datasets used and/or analyzed during the current study are available from the corresponding author upon reasonable request.

Competing interests

The authors declare that they have no competing interests.

Funding

This work was supported in part by the Keio Gijuku Fukuzawa Memorial Fund for the Advancement of Education and Research.

Authors' contributions

KT conceived and designed the experiments; LN performed the experiments. MS performed the sensory evaluation, analyzed the data, and wrote the paper with critical inputs from all authors.

Acknowledgements

Not applicable.

References

1. Grohmann B, Spangenberg ER, Sprott DE (2007) The influence of tactile input on the evaluation of retail product offerings. J Retailing 83 (2):237–245. https://doi.org/10.1016/j.jretai.2006.09.001
2. Yazdanparast A, Spears N (2013) Can consumers forgo the need to touch products? An investigation of nonhaptic situational factors in an online context. Psychol Mark 30 (1):46–61. https://doi.org/10.1002/mar.20588
3. Schifferstein HNJ (2006) The perceived importance of sensory modalities in product usage: A study of self-reports. Acta Psychol 121 (1):41–64. https://doi.org/10.1016/j.actpsy.2005.06.004
4. Jansson-Boyd CV (2011) Touch matters: Exploring the relationship between consumption and tactile interaction. Soc Semiot 21 (4):531–546: Abs.. https://doi.org/10.1080/10350330.2011.591996
5. Fishel JA, Loeb GE (2012) Sensing tactile microvibrations with the BioTac – Comparison with human sensitivity, vol 2012 4th IEEE RAS & EMBS International Conference Biomedical Robotics and Biomechatronics (BioRob): 1122–1127. https://doi.org/10.1109/BioRob.2012.6290741
6. Lin W, Wang B, Peng G, Shan Y, Hu H, Yang Z (2021) Skin-inspired piezoelectric tactile sensor array with crosstalk-free row+column electrodes for spatiotemporally distinguishing diverse stimuli. Adv Sci (Weinh) 8 (3):2002817. https://doi.org/10.1002/advs.202002817

7. Zheng W, Wang B, Liu H, Wang X, Li Y, Zhang C (2019) Bio-inspired magnetostrictive tactile sensor for surface material recognition. IEEE Trans Magn 55 (7):1–7. https://doi.org/10.1109/TMAG.2019.2898546
8. Dong S, Yuan W, Adelson EH (2017) Improved GelSight tactile sensor for measuring geometry and slip, vol 2017. IEEE Publications/RSJ International Conference on Intelligent Robots and Systems:137-144. https://doi.org/10.1109/IROS.2017.8202149
9. Wan Y, Qiu Z, Hong Y, Wang Y, Zhang J, Liu Q, Wu Z, Guo CF (2018) A highly sensitive flexible capacitive tactile sensor with sparse and high-aspect-ratio microstructures. Adv Electron Mater 4 (4). https://doi.org/10.1002/aelm.201700586
10. Peyre K, Tourlonias M, Bueno MA, Spano F, Rossi RM (2019) Tactile perception of textile surfaces from an artificial finger instrumented by a polymeric optical fibre. Tribol Int 130:155–169. https://doi.org/10.1016/j.triboint.2018.09.017
11. Fu J, Li F (2015) A forefinger-like tactile sensor for elasticity sensing based on piezoelectric cantilevers. Sens Actuators A 234:351–358. https://doi.org/10.1016/j.sna.2015.09.031
12. Wang Y, Ding W, Mei D (2021) Development of flexible tactile sensor for the envelop of curved robotic hand finger in grasping force sensing. Measurement 180. https://doi.org/10.1016/j.measurement.2021.109524
13. Niu H, Gao S, Yue W, Li Y, Zhou W, Liu H (2020) Highly morphology-controllable and highly sensitive capacitive tactile sensor based on epidermis-dermis-inspired interlocked asymmetric-nanocone arrays for detection of tiny pressure. Small 16 (4):e1904774. https://doi.org/10.1002/smll.201904774
14. Zhu P, Wang Y, Wang Y, Mao H, Zhang Q, Deng Y (2020) Flexible 3D architectured piezo/thermoelectric bimodal tactile sensor array for E-Skin application. Adv Energy Mater 10 (39). https://doi.org/10.1002/aenm.202001945
15. Thieulin C, Pailler-Mattei C, Vargiolu R, Lancelot S, Zahouani H (2017) Study of the tactile perception of bathroom tissues: Comparison between the sensory evaluation by a handfeel panel and a tribo-acoustic artificial finger. Colloids Surf B Biointerfaces 150 (1):417–425. https://doi.org/10.1016/j.colsurfb.2016.11.006
16. Sankar S, Balamurugan D, Brown A, Ding K, Xu X, Low JH, Yeow CH, Thakor N (2021) Texture discrimination with a soft biomimetic finger using a flexible neuromorphic tactile sensor array that provides sensory feedback. Soft Robot 8 (5):577–587. https://doi.org/10.1089/soro.2020.0016
17. Asaga E, Takemura K, Maeno T, Ban A, Toriumi M (2013) Tactile evaluation based on human tactile perception mechanism. Sens Actuators A 203:69–75. https://doi.org/10.1016/j.sna.2013.08.013
18. Chen S, Ge S, Tang W, Zhang J, Chen N (2015) Tactile perception of fabrics with an artificial finger compared to human sensing. Text Res J 85 (20):2177–2187. https://doi.org/10.1177/0040517515586164
19. Ito F, Kenjiro T (2021) A model for estimating tactile sensation by machine learning based on vibration information obtained while touching an object. Sensors (Basel) 21 (23):7772.

https://doi.org/10.3390/s21237772

20. Nobuyama L, Kurashina Y, Kawauchi K, Matsui K, Takemura K (2018) Tactile estimation of molded plastic plates based on the estimated impulse responses of mechanoreceptive units. Sensors (Basel) 18 (5):1588. https://doi.org/10.3390/s18051588
21. Hosoda K, Tada Y, Asada M (2006) Anthropomorphic robotic soft fingertip with randomly distributed receptors. Robot Auton Syst 54 (2):104–109. https://doi.org/10.1016/j.robot.2005.09.019
22. Huang S, Wu H (2021) Texture recognition based on perception data from a bionic tactile sensor. Sensors (Basel) 21 (15):5224. https://doi.org/10.3390/s21155224
23. Johansson RS, Landström U, Lundström R (1982) Responses of mechanoreceptive afferent units in the glabrous skin of the human hand to sinusoidal skin displacements. Brain Res 244 (1):17–25. https://doi.org/10.1016/0006-8993(82)90899-x
24. Gescheider GA, Bolanowski SJ, Hardick KR (2001) The frequency selectivity of information-processing channels in the tactile sensory system. Somatosens Mot Res 18 (3):191–201. https://doi.org/10.1080/01421590120072187
25. Bolanowski SJ, Gescheider GA, Verrillo RT, Checkosky CM (1988) Four channels mediate the mechanical aspects of touch. J Acoust Soc Am 84 (5):1680–1694. https://doi.org/10.1121/1.397184
26. Taylor MM, Lederman SJ, Gibson RH (1973) Tactual perception of texture. In: Handbook of perception, vol 3. Academic Press, New York
27. Shirado H, Maeno T (2005) Modeling of human texture perception for tactile displays and sensors, vols 629–630. First Joint Eurohaptics Conference and Symposium on Haptic Interfaces for Virtual Environment and Teleoperator Systems. World Haptics Conference. https://doi.org/10.1109/WHC.2005

Figures

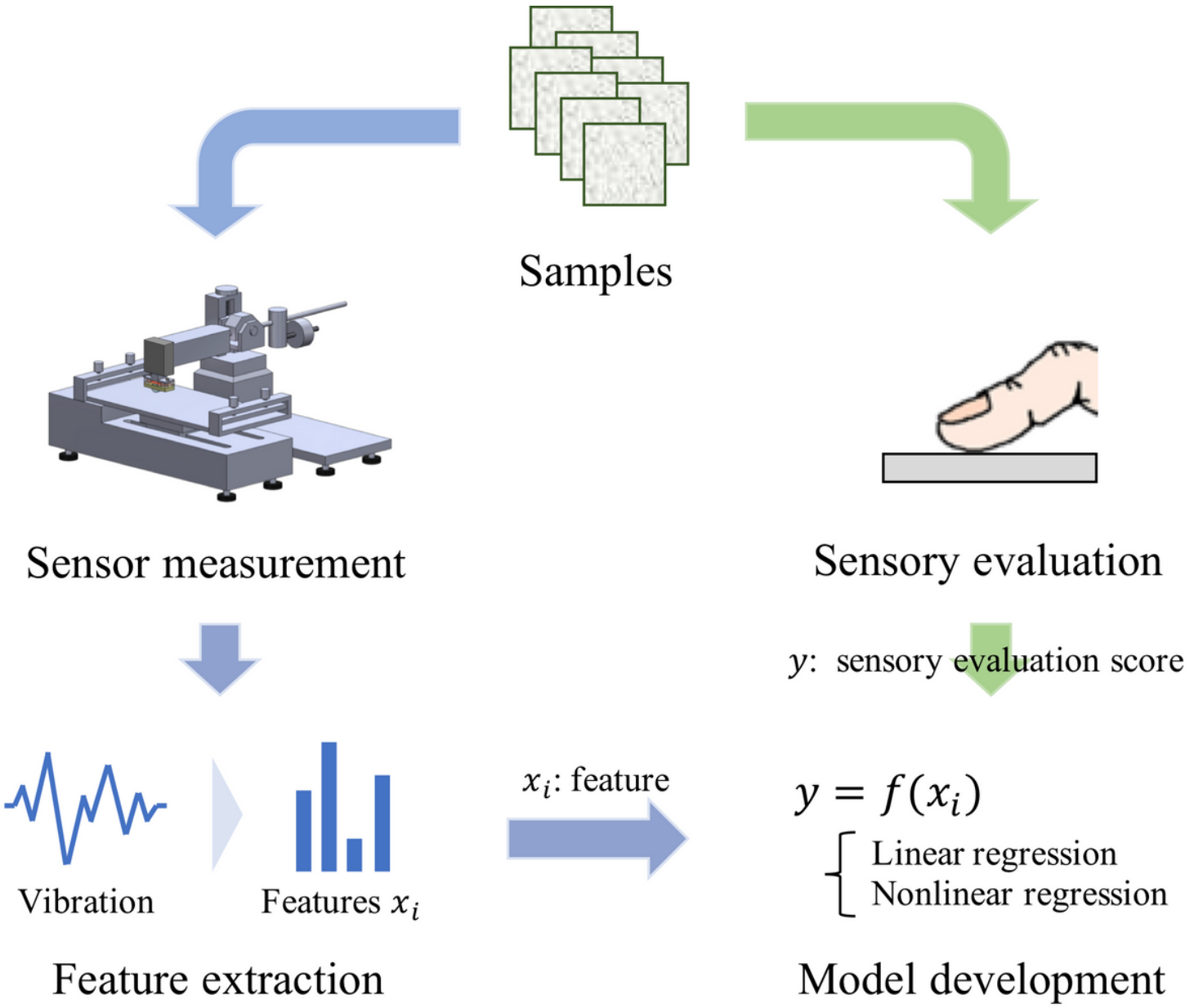

Figure 1

Structure of this study

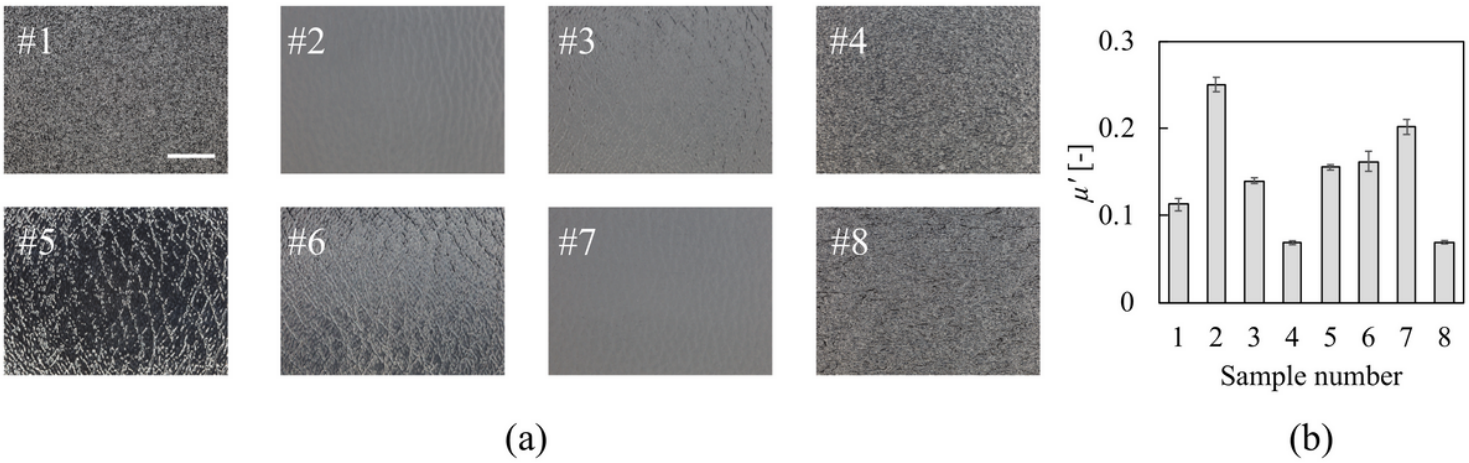

Figure 2

Information of plastic plates

(a) The enlarged views of test samples (Scale bar: mm)

(b) dynamic friction coefficient, μ' (mean ± SD, n = 10).

The plates were as follows: #1, polystyrene; #2, unknown; #3, polypropylene; #4, polyethylene; #5, polycarbonate; #6, polymethylmethacrylate; #7, unknown; #8, polyethylene

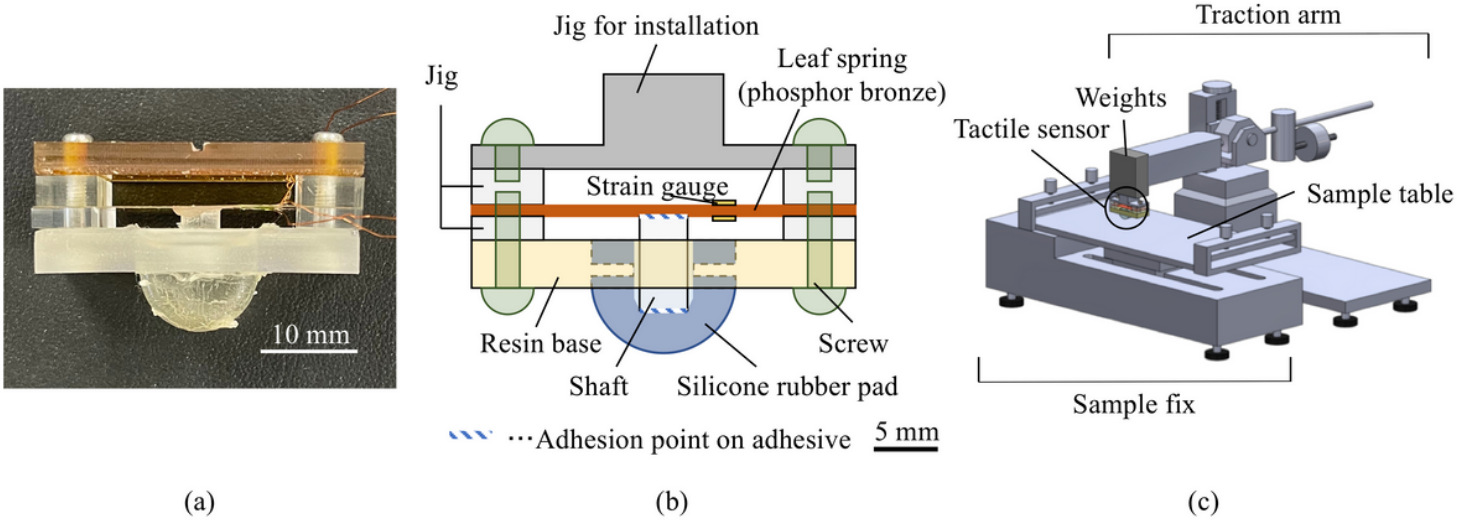

Figure 3

Tactile sensing system with developed tactile sensor

(a) Actual image of the tactile sensor

(b) Schematic diagram of the tactile sensor structure

(c) Overall view of the sensing system

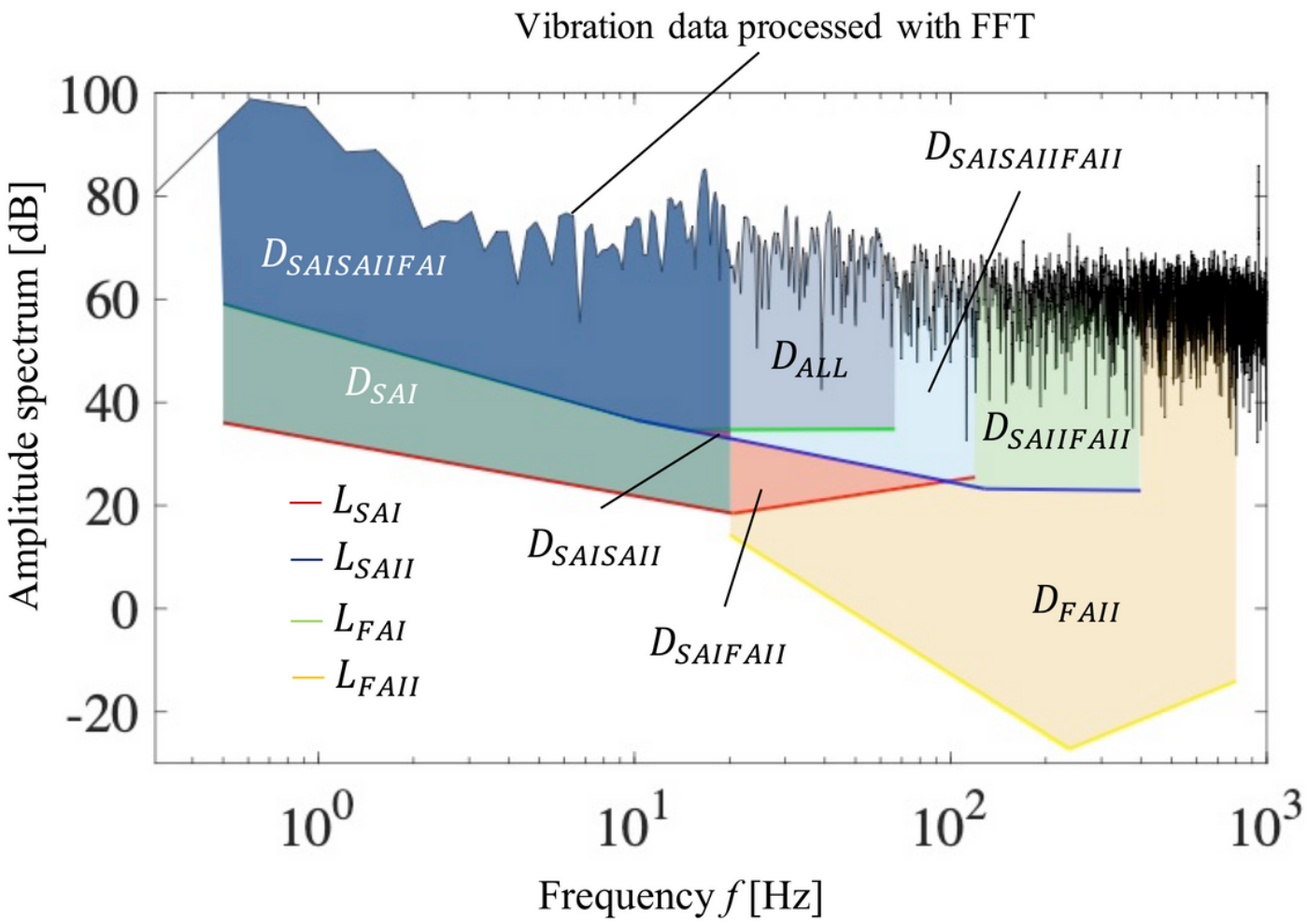

Figure 4

Conceptual diagram for calculation of the features

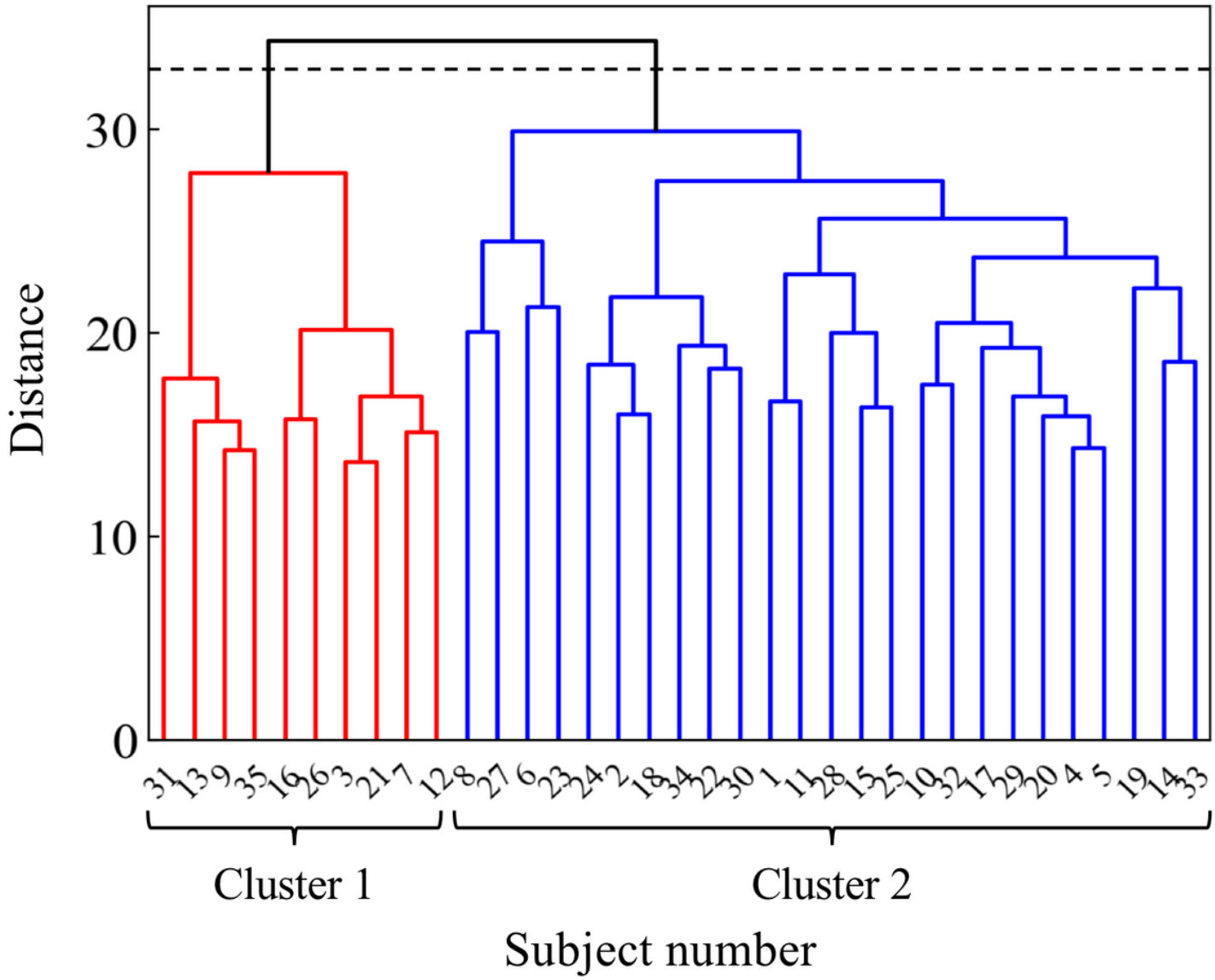

Figure 5

Dendrogram obtained from cluster analysis

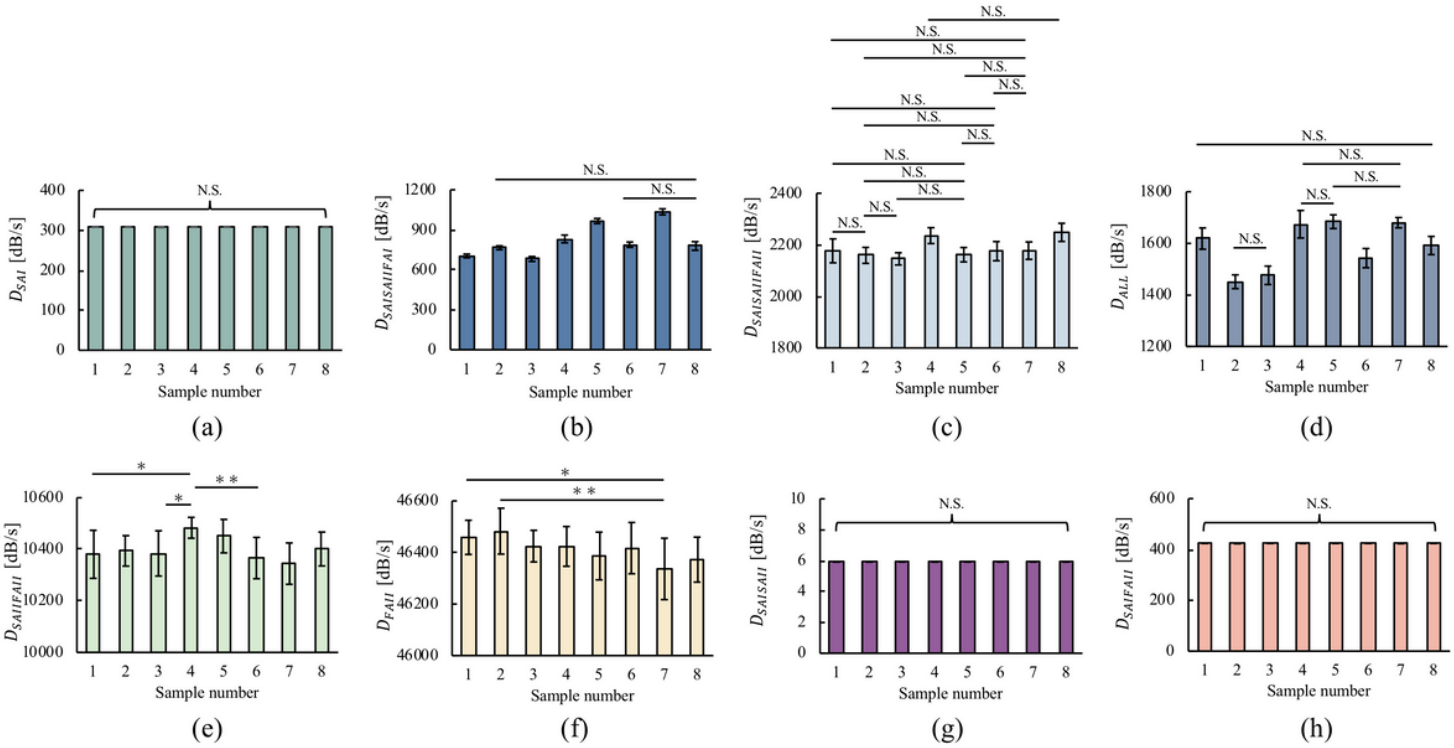

Figure 6 Results of feature calculation for the eight samples

(a) D_{SAI} (b) $D_{SAISAIIFAI}$ (c) $D_{SAISAIIFAII}$ (d) D_{ALL} (e) $D_{SAIIFAII}$ (f) D_{FAII} (g) $D_{SAISAII}$

(h) $D_{SAIFAII}$

(mean ± SD, $n = 11$, NS : No significant difference at 5% significance probability, *: $p <$ 0.05, **: $p < 0.01$)

Figure 6

"See image above for figure legend"

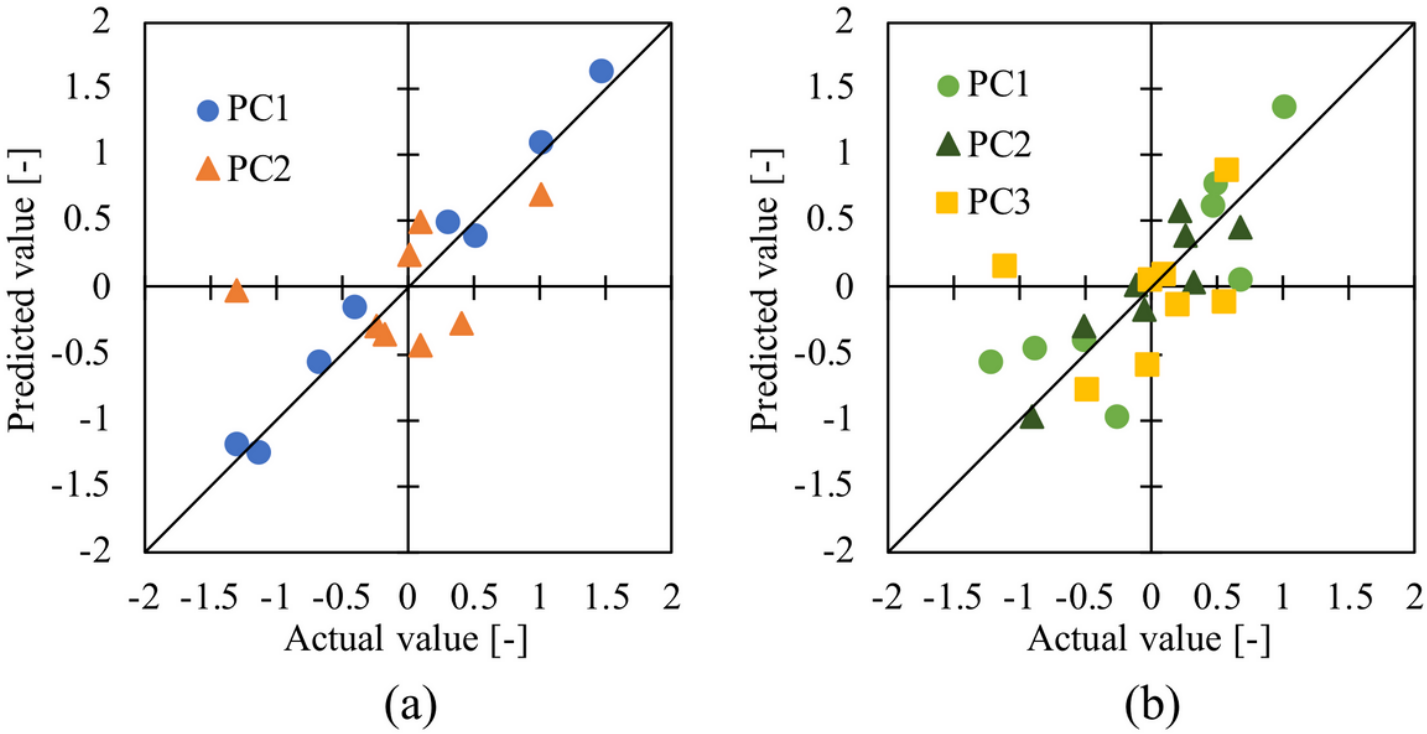

Figure 7

Relationship between the actual value and the predicted value

(a) Cluster 1 (b) Cluster 2

Supplementary Files

This is a list of supplementary files associated with this preprint. Click to download.

- supplement.docx
- FigureS1.pdf
- FigureS2outputd.pdf
- FigureS3mechanoreceptors.pdf
- FIgureS4mechanoreceptorthreshold.tiff
- FigureS5asagafeatures.tiff